The International Journal of Engineering and Science (IJES)
|| Volume || 9 || Issue || 10 || Series I || Pages || PP 01-09 || 2020 ||
ISSN (e): 2319-1813 ISSN (p): 20-24-1805

Distribution Characteristics of Dynamic Pressure In Nozzle Flow Meter

Sen-Da Qi, Jiang-Bo Tong, Feng Wang, Gong He, Shu-Yuan Wang, Guo-Qing Zhao, Zi-Yan Hu, Cheng-Xi Chai,
College of Mechanical Engineering, Quzhou University, Quzhou, 324000, China;

---------- ***ABSTRACT***----------
In order to research the internal dynamic pressure distribution characteristics of nozzle flowmeter, FLUENT software is used to simulate the nozzle flowmeter under different working conditions. Therefore, the internal dynamic pressure data of nozzle flowmeter under different flow rates are obtained. The results show that the dynamic pressure distribution is affected by the flow rate, and the nozzle flowmeter shows different degrees of motion on different fluid surface lines, so the dynamic pressure characteristics of each fluid surface line will still be different. This study has a certain significance for understanding the dynamic pressure distribution in the nozzle flowmeter and improving the measurement performance of the nozzle flowmeter.
KEYWORDS*: Nozzle flowmeter, numerical calculation, flow rate, dynamic pressure distribution.*

Date of Submission: 30-09-2020 Date of Acceptance: 13-10-2020

I. INTRODUCTION

Nozzle flowmeter has the advantages of simple structure, convenient installation, stable performance, short straight pipe length, high temperature and high pressure resistance, impact resistance and so on. Therefore, it is suitable for the flow measurement of oil, steam, water and other media. Then, the measurement principle of nozzle flowmeter is based on the throttling principle of fluid mechanics. When the fluid filled with the pipeline flows through the nozzle in the pipe, the flow rate will form local contraction in the nozzle, thus the flow rate will be accelerated and the static pressure will be reduced. Therefore, the pressure drop or differential pressure[1] will be generated before and after the nozzle. The greater the flow rate of the medium, the greater the pressure difference before and after the nozzle. So, the fluid flow rate can be measured by measuring the pressure difference[2]. Luo Zhaoqiang, Ya Yunqi and others carried out research on the inspection and detection of an ISA1932 nozzle steam flowmeter[3,4], and found that A-type pulsed ultrasound was not suitable for the detection of ISA1932 type flowmeter due to the length of the straight section of the short section of the ring chamber of the flowmeter and the welding joint form of the two ring chamber nipples of the flowmeter. Wang Yue and others found that the accuracy of orifice flowmeter was not high and in order to study the appropriate pressure taking position of nozzle flowmeter[5-7], numerical simulation of nozzle flowmeter under different working conditions was carried out by FLUENT software. It was found that the pressure and velocity near the nozzle in the flow field had obvious fluctuations. For example, the closer to the nozzle, the greater the range of pressure and velocity change. Liu Hongsheng's team carried out relevant tests and calculations on the 6D front straight pipe section of the nozzle flowmeter, and obtained the preliminary conclusion of the application system by using the calibration test and flow field calculation[8], and this paper studies the dynamic pressure distribution characteristics inside the nozzle flowmeter.

II. RESEARCH OBJECT AND METHOD

2.1 physical model

The upstream face of the nozzle flowmeter consists of a perpendicular plane to the axis, a 1/4 elliptical contraction section, a cylindrical throat and possible grooves or inclined angles, as shown in Figure 1. Its total length is 250 mm, the total width is 358 mm, and the nominal diameter is 213 mm.

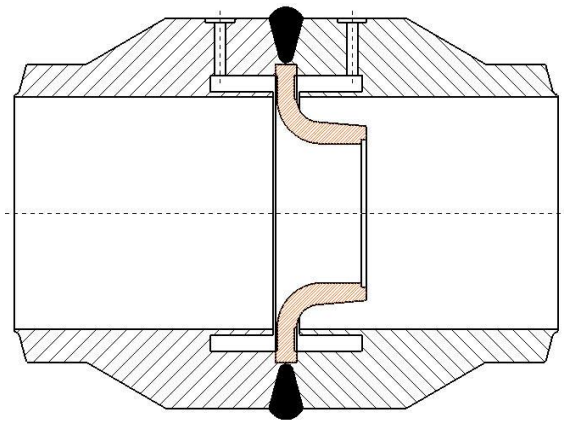

Figure 1 overall structure diagram of nozzle flow meter

2.2 governing equations

According to fluid mechanics, in rectangular coordinates, for incompressible viscous fluid, its law of motion is controlled by Navier Stokes equations. The forms of continuity equation and momentum equation are as follows.

$$\frac{\partial \mu}{\partial x}+\frac{\partial v}{\partial y}=0 \tag{1}$$

$$\rho u\frac{\partial u}{\partial x}+\rho v\frac{\partial u}{\partial y}=-\frac{\partial p}{\partial x}+\frac{\partial}{\partial y}\left(\eta\frac{\partial u}{\partial y}\right) \tag{2}$$

2.3 calculation method

At standard atmospheric pressure, by setting the fluid attribute, the fluid medium is water, and the density is $\rho=1kg/m^3$ and dynamic viscosity is $\eta=0.001Pa\bullet s$. So, in order to get exact calculation to a higher degree, the simple scheme of coupling pressure term and velocity term are set. In the same way, in order to remove the influence of dimension effect of standard nozzle forging on the calculation results, make the $\mu=U$, $v=0$. At the same time, set the standard nozzle core to the condition of no penetration and no slip, as $\mu=U$, $v=0$.

2.4 calculation scheme

The study to the face identification of key surface of nozzle flowmeter has great significance to internal flow characteristics. The identification of the four surfaces is shown in Figure 2, where Face 1 represents the upstream face of the nozzle, Face 2 represents the downstream outlet surface of the nozzle, Face 3 represents the outlet surface of the nozzle flowmeter, and Face 4 represents the horizontal plane passing through the central axis of the nozzle flowmeter. What'more, the surface line identification of nozzle flowmeter is shown in Figure 3, where Line 11 is the center line of flowmeter.

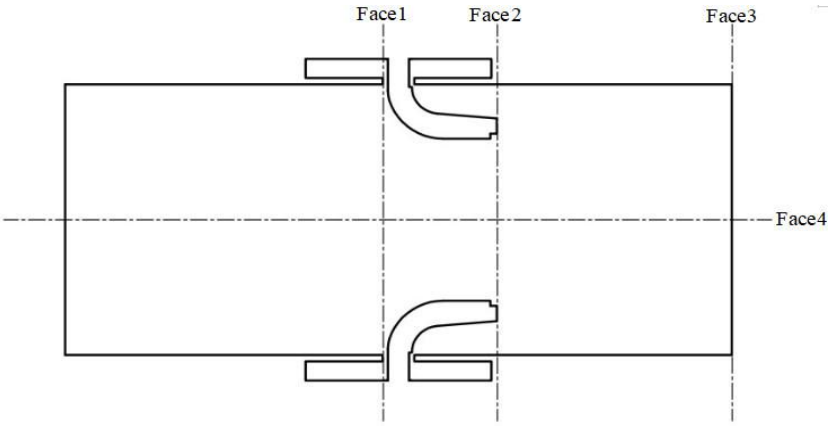

Figure 2 Identification of nozzle flowmeter surface

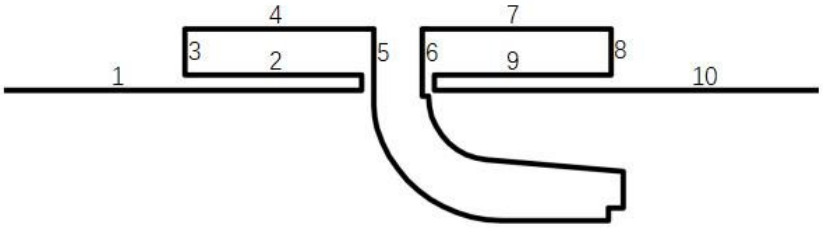

Figure 3 surface line identification of nozzle flowmeter

Overall, in order to study the dynamic pressure distribution in the nozzle flowmeter under different flow rates. In this study, eight kinds of stable flow values will be taken, which are 5 m^3/h, 25 m^3/h, 50 m^3/h, 125 m^3/h, 250 m^3/h, 500 m^3/h, 750 m^3/h and 1000 m^3/h respectively. The calculation scheme is shown in Table 1.

Table 1 Calculation Scheme

Calculation scheme(case)	No.1	No.2	No.3	No.4	No.5	No.6	No.7	No.8
Working condition flow(m^3/h)	5	25	50	125	250	500	750	1000

For the study of four identification surfaces, the steady flow values are taken as 5 m^3/h, 25 m^3/h, 125 m^3/h and 750 m^3/h. Among them, 5 m^3/h refers to ultra-small flow condition, 25 m^3/h refers to small flow condition, 125 m^3/h medium and small flow condition, and 750 m^3/h large flow condition.

III. Result analysis

The (a), (b), (c) and (d) in the following cloud images represent Face 1, Face 2, Face 3 and Face 4 respectively. The (a), (b), (c), (d), (E), (f), (g), (H), (I), (J) and (k) in line diagram denote Line 1, Line 2, Line 3, Line 4, Line 5, Line 6, Line 7, Line 8, Line 9, Line 10 and Line 11 respectively.

3.1 Dynamic pressure distribution

The distribution of dynamic pressure under ultra-small flow rate (5 m^3/h) is shown in Figure 4. When the inlet flow rate is 5 m^3/h, the maximum dynamic pressure of Face 1 is 0.0015 Pa at the center of the surface , as well as the minimum dynamic pressure appears in the outer ring of the face, with the value of 0 Pa, and the dynamic pressure is gradually reduced from the center ring layer; the maximum dynamic pressure of Face 2 is 0.0045Pa at the outer circle of the center surface, and the minimum dynamic pressure appears in the outer ring of the surface, with the value of 0.0045 Pa, and the overall trend of dynamic pressure decreases from the middle to the outside. The maximum dynamic pressure of Face 3 appears at the center of the face, and its value is 0.0036 Pa. The minimum dynamic pressure appears in the outer ring of the face, and the value is 0 Pa; the maximum dynamic pressure of Face 4 appears at the positive center of the nozzle, which is 0.004 Pa.The minimum dynamic pressure appears on the inlet, step and outlet surfaces of the nozzle flowmeter, and its value is 0 Pa.

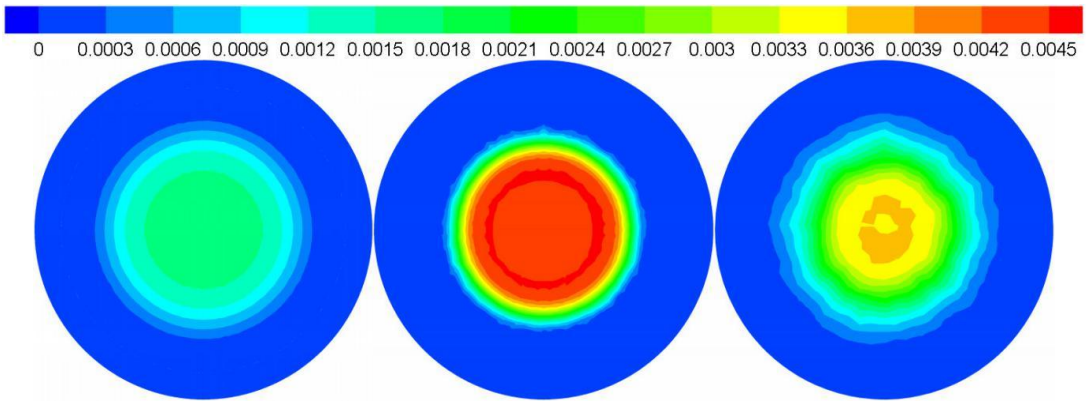

(a) (b) (c)

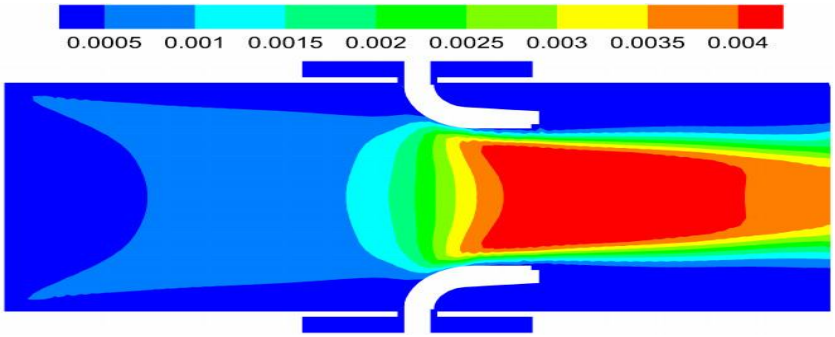

(d)

Figure 4 dynamic pressure distribution under ultra-small flow rate (5 m^3/h)

The distribution of dynamic pressure at small flow rate (25 m^3/h) is shown in Figure 5. When the inlet flow rate is 25 m^3/h, the maximum dynamic pressure of Face 1 appears at the positive center of the upstream face of the nozzle, which is 0.03 Pa, and the minimum dynamic pressure appears in the outermost circle of the nozzle, with the value of 0 Pa, and the dynamic pressure is gradually reduced from the central layer to the outside; The maximum dynamic pressure of Face 2 appears at the positive center of the downstream outlet surface of the nozzle, which is 0.09 Pa, and the minimum dynamic pressure appears in the outermost circle of the nozzle, with the value of 0 Pa. The dynamic pressure on Face 2 decreases gradually from the center ring layer outward, and the dynamic pressure in the middle is the most concentrated; Face 3 has the maximum dynamic pressure at the positive center of the nozzle flowmeter outlet surface, the value is 0.06 Pa, and the minimum dynamic pressure appears in the outermost circle of the surface, which value is 0 Pa, and the dynamic pressure is gradually reduced from the center ring layer outward.The maximum dynamic pressure of Face 4 is 0.09 Pa when the fluid flows out of the nozzle center, and the minimum dynamic pressure appears at the step and outlet of the nozzle flowmeter, and its value is 0 Pa. The dynamic pressure at the inlet area of the standard nozzle core is relatively small, and the dynamic pressure change at the outlet area is obvious, and the dynamic pressure change has hierarchical change.

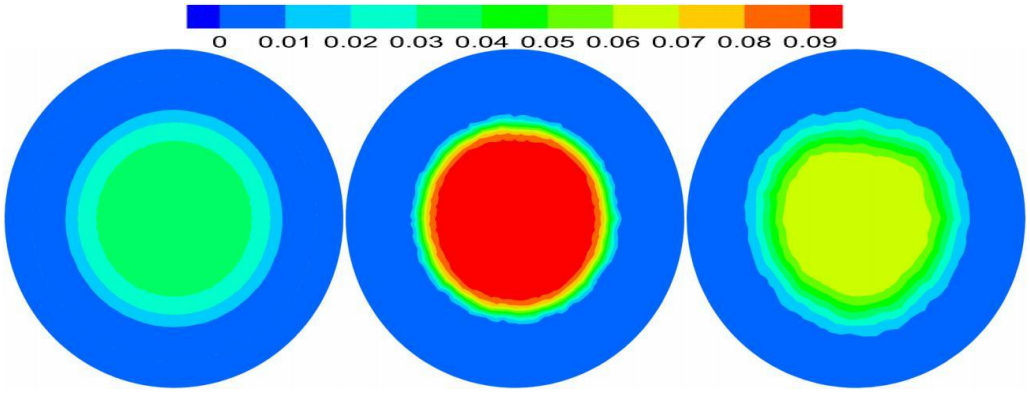

(a) (b) (c)

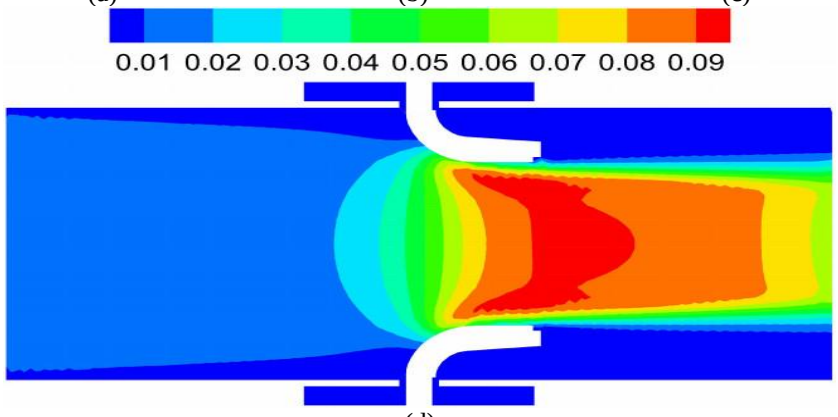

(d)

Figure 5 dynamic pressure distribution at small flow rate (25 m^3/h)

The distribution of dynamic pressure at small and medium flow rate (125 m^3/h) is shown in Figure 6. When the inlet flow rate is 125 m^3/h,the maximum dynamic pressure of Face 1 is 0.8 Pa at the positive center of the surface, and the minimum dynamic pressure appears in the outermost circle of the face, with the value of 0 Pa, and the dynamic pressure is gradually reduced from the central circle to the outside; the maximum dynamic pressure of Face 2 appears at the positive center of the surface, and its value is 2 Pa, and the minimum dynamic pressure appears in the outermost circle of the face, and its value is 0 Pa. The dynamic pressure on Face 2 decreases gradually from the central circle layer outward, and the dynamic pressure in the middle is the most concentrated;the maximum dynamic pressure of Face 3 is 1.4 Pa at the outlet of the nozzle flowmeter, and the minimum dynamic pressure appears in the outermost circle of the nozzle flowmeter, which is 0 Pa. There are some concentrated dynamic pressures in some areas, but they occupy a small Part of the total area;the maximum dynamic pressure of Face 4 appears at the inflection point of nozzle arc, the value is 2.2 Pa, and the minimum dynamic pressure appears at the step and outlet of nozzle flowmeter, the value is 0 Pa, and comPared with the flow rate of 25 m^3/h, the dynamic pressure at the outlet of the standard nozzle core gradually starts to concentrate from a large area, but the dynamic pressure change is still a class change. The closer to the outlet of the standard nozzle forging, the smaller the dynamic pressure.

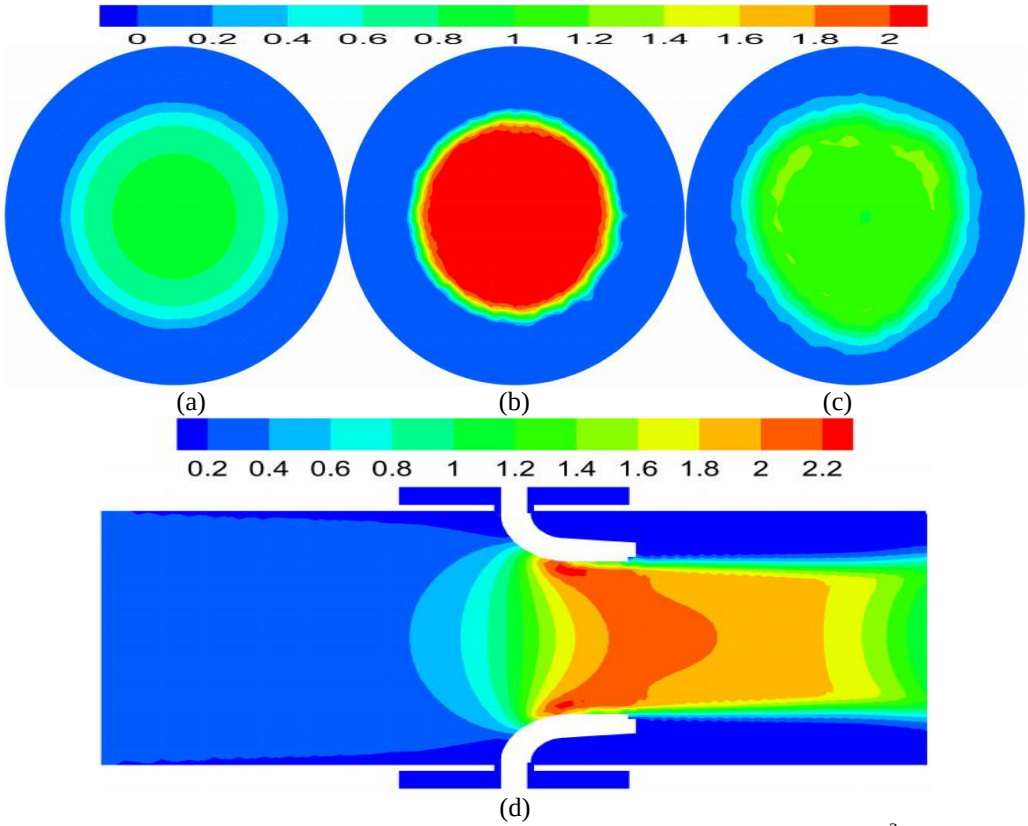

Figure 6 dynamic pressure distribution at small and medium flow (125 m^3/h)

The distribution of dynamic pressure at large flow rate (750 m^3/h) is shown in Figure 7. When the inlet flow rate is 750 m^3/h, the maximum dynamic pressure of Face 1 appears at the center of the upstream face of the nozzle, which is 20 Pa, and the minimum dynamic pressure appears in the outermost circle of the nozzle with the value of 0 Pa, and there are only three kinds of dynamic pressure distribution;the maximum dynamic pressure of Face 2 appears at the positive center of the downstream outlet surface of the nozzle, which is 70 Pa, and the minimum dynamic pressure appears in the outermost circle of the nozzle with the value of 0 Pa, and the dynamic pressure is gradually reduced from the central ring layer to the outside;the maximum dynamic pressure of Face 3 appears in the outer circle of the outlet center of the nozzle flowmeter, which is 40 Pa, and the minimum dynamic pressure appears in the outermost circle of this surface, which is 0 Pa, and the dynamic pressure of small area in the center of this surface is 20 Pa;the maximum dynamic pressure of Face 4 appears at the corner of nozzle arc, with the value is 80 Pa, and the minimum dynamic pressure is 0 Pa at the step and outlet of nozzle flowmeter. It can be seen from the figure that the dynamic pressure on the area around the standard nozzle core of key components is changeable, and even the dynamic pressure on the Path until the liquid flows out of the standard nozzle core also has many changes.

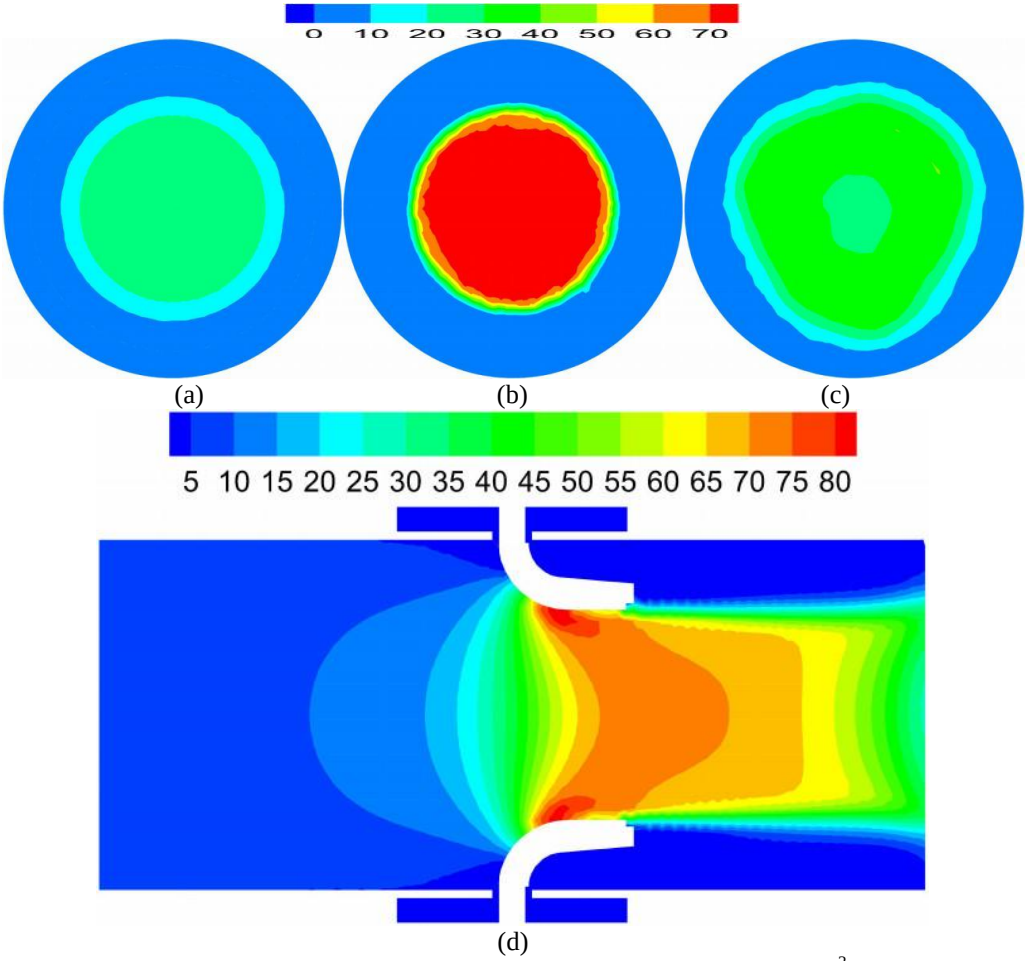

Figure 7 dynamic pressure distribution at large flow rate (750 m^3/h)

3.2 Dynamic pressure distribution at boundary

The dynamic pressure distribution of the nozzle flowmeter at the boundary is shown in Figure 8. The nozzle flowmeter shows different degrees of motion on different fluid surfaces, so the dynamic pressure characteristics of each fluid surface will still be different.

In Figure 8(a), the dynamic pressure on Line 1 increases gradually with the increase of flow rate. When the flow rate is less than 125 m^3/h, the dynamic pressure is basically kept at 0 kPa. When the flow rate is 250 m^3/h, the dynamic pressure is about 1 kPa. When the flow rate is 500 m^3/h and 750 m^3/h, the dynamic pressure fluctuates around 3 kPa and 6 kPa respectively. When the flow rate is 1000 m^3/h, the dynamic pressure gradually decreases from 16 kPa, but the dynamic pressure on Line 1 is still at a high value. When l is less than 0.7, the dynamic pressure is fluctuating. When l is between 0.7 and 1.0, the dynamic pressure on Line 1 gradually decreases to zero under large flow conditions.

In Figure 8(b), when l is less than 0.8, Line 2 is almost free from any dynamic pressure at eight flow rates. When l is 0.8 to 1.0, the small flow is not subjected to dynamic pressure, and the dynamic pressure value is 0 kPa. When the flow rate is greater than 125 m^3/h, the dynamic pressure on Line 2 changes. When the flow rate is 500 m^3/h, the dynamic pressure on Line 2 is the largest and gradually increases to 0.0055 kPa. When the flow rate is 750 m^3/h, 250 m^3/h and 1000 m^3/h, the dynamic pressure of Line 2 gradually increases to 0.0018 kPa, 0.0008 kPa and 0.0005 kPa, respectively.

In Figure 8(c), Line 3 is almost free from dynamic pressure at low flow rates. When the flow rate is more than 250 m^3/h, the dynamic pressure graph is similar to the line chart. When the flow rate is 500 m^3/h, 750 m^3/h and 1000 m^3/h, the dynamic pressure on Line 3 gradually increases and tends to be stable, and then rises rapidly to the peak value of dynamic pressure of 0.000046 kPa, 0.00005 kPa and 0.00003 kPa, respectively. Then, with the increase of l, the dynamic pressure on Line 3 decreases to 0.

In Figure 8(d), the dynamic pressure on Line 4 is in the form of aperiodic oscillation. When the flow rate is less than 125 m^3/h, the dynamic pressure of Line 4 is 0 kPa. When the flow rate is 250 m^3/h, the dynamic pressure has a small fluctuation. When the flow rate is 500 m^3/h, 750 m^3/h and 1000 m^3/h, the dynamic pressure on Line 4 is the maximum at the flow rate of 500 m^3/h. When l is greater than 0.8, the dynamic pressure

decreases gradually to 0 kPa.

In Figure 8 (e), when l is less than 0.4, Line 5 is not subjected to dynamic pressure at eight flow rates. When l is greater than 0.4, the dynamic pressure is gradually affected. When the flow rate is 250 m^3/h, the dynamic pressure is not obvious. When the flow rate is 500 m^3/h, the dynamic pressure is gradually subjected to the dynamic pressure. However, when the l is 0.85, the dynamic pressure begins to decrease, dropping to the lowest point, and then gradually increases to 0.05 kPa. When the flow rate is 750 m^3/h and 1000 m^3/h, the overall trend of dynamic pressure is upward, but the dynamic pressure of 1000 m^3/h is more obvious, especially when l is greater than 0.7, the dynamic pressure changes, and the dynamic pressure of Line 4 rises rapidly to 0.12 kPa.

In Figure 8(f), when the flow rate is lower than 250 m^3/h, the dynamic pressure on Line 6 is 0. When the flow rate is higher than 250 m^3/h, the dynamic pressure trend of Line 6 is gradually increased to the highest point, and then a downward trend appears. When the flow is 500 m^3/h, the maximum dynamic pressure is 0.1 kPa; when the flow is 750 m^3/h, the maximum dynamic pressure is 0.3 kPa; when the flow is 1000 m^3/h, the maximum dynamic pressure is 1.5 kPa.

In Figure 8(g), when the flow rate is less than 250 m^3/h, the dynamic pressure on Line 7 is 0 kPa. When l is greater than 0.3, the dynamic pressure of Line 7 under medium and large flow rate is 0 kPa. When l is less than 0.3 and the flow rate is 500 m^3/h and 750 m^3/h, the dynamic pressure on Line 7 is relatively low. When the flow rate is 1000 m^3/h, the dynamic pressure fluctuation is obvious. The dynamic pressure on Line 7 rises rapidly from 0.022 kPa to the highest point of 0.15 kPa, and then decreases to 0 kPa.

In Figure 8(H), when the flow rate is less than 250 m^3/h, the dynamic pressure on Line 8 is almost close to 0 kPa. When the flow rate is 500 m^3/h, 750 m^3/h and 1000 m^3/h, the dynamic pressure trend is similar, which is gradually increased, then tends to be stable, and finally decreases with the increase of L. When l is 0.6 to 0.8, the dynamic pressure stability values of 500 m^3/h, 750 m^3/h and 1000 m^3/h are 0.18 kPa, 0.3 kPa and 1.5 kPa, respectively. When the flow rate is 1000 m^3/h, the rising trend of dynamic pressure is different from that of 500 m^3/h and 750 m^3/h when l is less than 0.6.

In Figure 8(I), when the flow rate is lower than 750 m^3/h, the dynamic pressure is less obvious, almost all of which fluctuate slightly around 0 kPa, and then tend to be stable. When l is 0 and the flow rate is 1000 m^3/h, the dynamic pressure on Line 9 is the maximum, and the dynamic pressure value reaches 0.16 kPa. Then the dynamic pressure decreases and increases. When l is 1.8, it reaches the peak point of dynamic pressure again, and the dynamic pressure is 0.05 kPa. Then, with the increase of l, the dynamic pressure decreases to 0 kPa.

In Figure 8(J), the fluctuation amplitude of Line 10 is small under small flow. When the flow rate is 125 m^3/h, the maximum dynamic pressure is 0.1 kPa. When the flow rate is less than 125 m^3/h, the dynamic pressure on Line 10 is 0 kPa. When the flow rate is 250 m^3/h, there is a small change in Line 10. The maximum dynamic pressure is 0.3 kPa when l is between 0.8 and 0.9. When the flow rate is 500 m^3/h, the dynamic pressure gradually increases to the highest point, and then decreases to close to 0 kPa, and the maximum dynamic pressure is 1.5 kPa. When the flow rate is 750 m^3/h and l is less than 0.6, the dynamic pressure on Line 10 fluctuates. When l is greater than 0.6, the dynamic pressure on Line 10 reaches the maximum value, which is 3.5 kPa, and then decreases to 0.5 kPa. When the flow rate is 1000 m^3/h, the dynamic pressure on Line 10 reaches three peaks, which l are 0.05, 0.25 and 0.9 respectively, and the values are 2 kPa, 0.9 kPa and 5.8 kPa respectively. When the flow rate is greater than 0.9, the dynamic pressure on Line 10 tends to decrease to 0.7 kPa.

In Figure 8(k), when the flow rate is less than 125 m^3/h, Line 11 is basically free from dynamic pressure and fluctuates around 0 kPa. When the flow rate is greater than 125 m^3/h, the dynamic pressure on Line 11 is obvious. When l is 0.62, the dynamic pressure of Line 11 begins to decrease under other large flow rates, while when the flow rate is 1000 m^3/h, the dynamic pressure of Line 11 continues to increase, and its maximum dynamic pressure reaches 130 kPa. When l is 0.62, the maximum dynamic pressure of 250 m^3/h, 500 m^3/h and 750 m^3/h is 7.5 kPa, 33 kPa and 75 kPa, respectively.

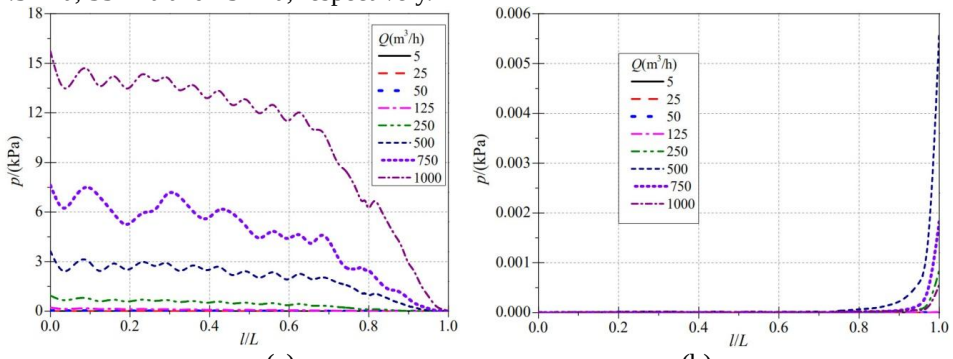

(a) (b)

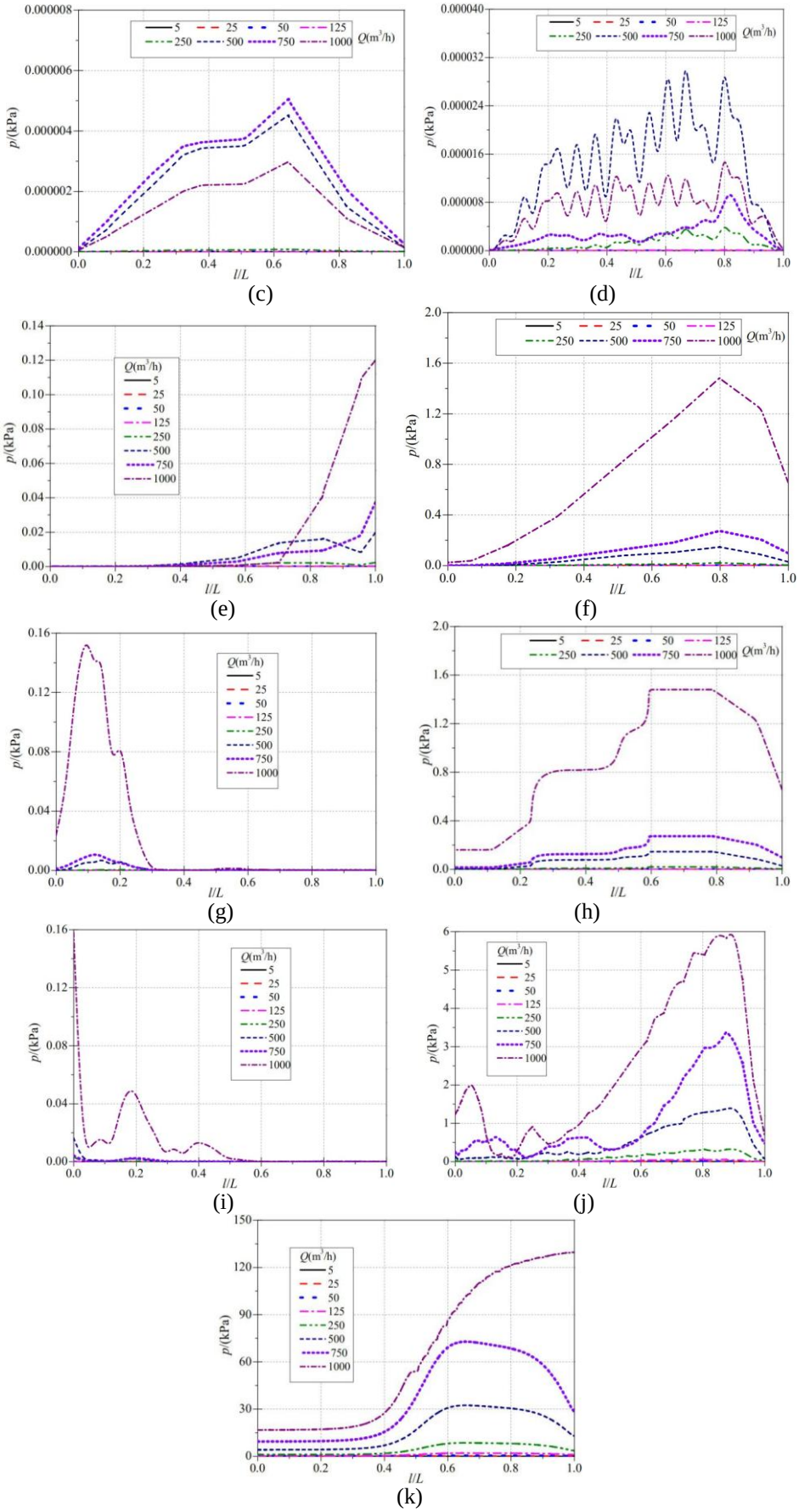

Figure 8 dynamic pressure distribution at boundary

IV. CONCLUSION

(1) It is found that the dynamic pressure distribution in the nozzle flowmeter is different under different flow rates. The maximum dynamic pressure appears in the positive center of the surface mark, and the minimum dynamic pressure appears in the outermost ring of the surface, and the trend of dynamic pressure decreases gradually from the center circle layer to the outside.

(2) The nozzle flowmeter shows different degrees of motion on different fluid surface lines, so the dynamic pressure characteristics of each fluid surface line will still be different, and the dynamic pressure on the surface line mark will change with the change of flow rate and total length.

(3) The dynamic pressure of the nozzle flowmeter is affected by the flow rate. In general, the dynamic pressure under large flow rate is relatively large.

ACKNOWLEDGEMENTS

The work was supported by the national college students' science and technology innovation project (No. 202011488018).

REFERENCE

[1]. Li Kangkang, Jia Yuming, Ge Sunan. Application of orifice throttling device[J]. Petrochemical Automation, 2010, 46(04): 60-63.
[2]. Wang Weiping. Application of automatic calculation of steam flow density in automatic control system[J]. Electromechanical Engineering Technology, 2011, 40(05): 61-64, 124.
[3]. Luo Zhaoqiang, Ya Yunqi, Dai Enxian, et al. Study on the detection method of ISA1932 nozzle steam flowmeter[J]. China Special Equipment Safety, 2019, 35(08): 19-24.
[4]. Hu Zhipeng, Zhao Yan. Verification comparison of manjie flowmeter on different gas flow standard devices[J]. China Metrology, 2007, (9): 59-60.
[5]. Wang Yue, Yan Yongfei, Zhou Jianping, et al. Numerical simulation of flow field and optimization of pressure taking position of nozzle flowmeter[J]. Contemporary Chemical Engineering, 2018, 47(10): 2161-2164, 2177.
[6]. Yang Xiaojun, Chen Baodong, Wang Jianqiao, et al. Development and prospect of differential pressure flowmeter[J]. Industrial Metrology, 2010, 20(3): 27-28.
[7]. Pan Zhen, Chen Baodong, Yan Yongfei, et al. Numerical simulation of surface pressure distribution of V-cone Flowmeter[J]. Energy Saving Technology, 2009, 27(4): 299-301.
[8]. Liu Hongsheng. Research on non standard application of nozzle flowmeter[J]. Valve, 2014, (02): 7-8, 23.

Sen-Da Qi, et. al. "Distribution Characteristics of Dynamic Pressure In Nozzle Flow Meter" The International Journal of Engineering and Science (IJES), 9(10), (2020): pp. 01-09.